Research Square

Preprints are preliminary reports that have not undergone peer review.
They should not be considered conclusive, used to inform clinical practice,
or referenced by the media as validated information.

AOV 100 Sessions: Regional Observations by the Asia-Oceania VLBI Group for Geodesy and Astrometry

Masafumi Ishigaki

ishigaki-m96bd@mlit.go.jp

Geospatial Information Authority of Japan https://orcid.org/0000-0002-6664-1949

Lucia McCallum

University of Tasmania https://orcid.org/0000-0002-7563-9488

Fengchun Shu

SHAO: Shanghai Astronomical Observatory Chinese Academy of Sciences

Tiege McCarthy

University of Tasmania https://orcid.org/0000-0001-9525-7981

Haruna Furui

Geospatial Information Authority of Japan

Takehiro Nishi

Geospatial Information Authority of Japan

Tetsuya Hara

Advanced Engineering Service Co., Ltd

Research Article

Keywords: Very Long Baseline Interferometry (VLBI), Asia-Oceania VLBI group for Geodesy and Astrometry (AOV), VLBI Global Observing System (VGOS)

Posted Date: November 12th, 2026

DOI: https://doi.org/10.21203/rs.3.rs-11233811/v1

License: This work is licensed under a Creative Commons Attribution 4.0 International License.
Read Full License

AOV 100 Sessions: Regional Observations by the Asia-Oceania VLBI Group for Geodesy and Astrometry

Masafumi Ishigaki, Geospatial Information Authority of Japan, ishigaki-m96bd@mlit.go.jp
Lucia McCallum, University of Tasmania, Australia, lucia.mccallum@utas.edu.au
Fengchun Shu, Shanghai Astronomical Observatory, sfc@shao.ac.cn
Tiege McCarthy, University of Tasmania, Australia, tiegem@utas.edu.au
Haruna Furui, Geospatial Information Authority of Japan, furui-h96pd@mlit.go.jp
Takehiro Nishi, Geospatial Information Authority of Japan, nishi-t96pc@mlit.go.jp
Tetsuya Hara, Advanced Engineering Service Co., Ltd, hara-t96xs@mlit.go.jp

Abstract

The Asia-Oceania VLBI Group for Geodesy and Astrometry (AOV) is a regional collaboration that supports geodetic and astrometric VLBI activities in the Asia–Oceania region and operates as a subgroup of the International VLBI Service for Geodesy and Astrometry (IVS). One purpose of the AOV collaboration is to secure ongoing expertise of the VLBI technique in the region. Shared obligations for governance and session planning, as well as for scheduling and correlation of the AOV sessions greatly support this goal. Since 2015, AOV has conducted regular legacy S/X VLBI sessions, reaching its 100th session in August 2025. In this study, we analyse these 100 sessions and compare the results of Earth Orientation Parameters (EOPs) and station coordinates with those derived from other IVS sessions. The station positions estimated from AOV sessions are comparable in accuracy to those from other networks, and the AOV sessions play an important role in stabilizing the positions of regional stations that primarily participate in AOV observations for geodetic purposes. The EOP estimates show moderate accuracy, which is consistent with the relatively limited size of the AOV network. We also investigate the potential impact of newly established stations in the region on the future performance of the AOV network. Finally, we introduce the ongoing AOV VGOS sessions and assess their expected impact in comparison with the current S/X sessions, with a view toward future developments of AOV sessions.

Keywords

Very Long Baseline Interferometry (VLBI), Asia-Oceania VLBI group for Geodesy and Astrometry (AOV), VLBI Global Observing System (VGOS)

1. Introduction

The International VLBI Service for Geodesy and Astrometry (IVS, Schl¨uter and Behrend 2007; Nothnagel et al. 2017) is an international collaboration of organisations which operate or support Very Long Baseline Interferometry (VLBI) components. Established in 1999 under the International Association of Geodesy (IAG) and the International Astronomical Union (IAU), the IVS coordinates a worldwide network of radio telescopes and analysis centres to provide highly accurate measurements of Earth Orientation Parameters (EOP), terrestrial and celestial reference frames, and station positions. It is composed of a broad international community of observing stations, correlators, analysis centres, technology development centres, and coordinating institutions distributed across many countries.

As a regional subgroup of the IVS, the Asia-Oceania VLBI Group for Geodesy and Astrometry (AOV) has actively contributed to collaboration in geodetic and astrometric VLBI within the Asia–Oceania region. The Asia-Oceania region is highly dynamic in geophysics and climate, with a large number of destructive earthquakes, tsunamis, typhoons and cyclones. In order to better understand the risks and reduce the effects of these phenomena, the AOV has an important role to play through measurement of tectonic plate motions, atmospheric variations and determination of the Geodetic Reference Frame for the region. In AOV sessions conducted within the region, network stations participate in the observations, while scheduling and correlation are also carried out by member organisations. These collaborations enable the participating institutions to share expertise in the group and improve their VLBI techniques, thereby enhancing the presence of the Asia–Oceania region within the global VLBI community. The AOV sessions also serve to anchor the positions of regional astronomical VLBI stations that do not regularly

participate in geodetic IVS sessions. AOV has coordinated its regular sessions since the first session in March 2015, and it achieved the 100th anniversary session in August 2025. This paper is the first to systematically summarize these results since a sufficient number of observations have been accumulated.

The structure of this paper is as follows. Section 2 introduces an overview of the activities of AOV, including its history from the establishment to current status, network stations, and session types. Section 3 describes how the AOV sessions are conducted in the processes of scheduling, observation, correlation and analysis. Section 4 presents the results of the sessions mainly focusing on uncertainty of obtained EOP and station positions, and Section 5 provides comparisons of the results with simulations and discussions of future AOV networks.

2. AOV Overview

2.1 Establishment and growth of the AOV

The concept of the AOV originated from informal discussions among several researchers from the Asia-Oceania region during the 21st European VLBI for Geodesy and Astrometry (EVGA) Meeting held in Finland in March 2013. Subsequently, at the preparatory meeting held after the IAG Scientific Assembly in Potsdam in September 2013, an agreement was reached to establish a regional VLBI community for the Asia–Oceania region. After the agreement, the establishment of AOV was formally approved at the 30th meeting of the IVS Directing Board. The inaugural AOV meeting was held in March 2014 during the IVS General Meeting in Shanghai, marking the formal launch of the organisation. In September 2014, the Terms of Reference were established, followed by the election of the first Chair in October 2014. A detailed description about this process

as well as the Terms of Reference can be found in Kurihara et al. (2015). The operational phase of the AOV began in March 2015, with the initiation of regular VLBI sessions coordinated by the group. The AOV consists of twelve organisations from five countries, including institutions from Japan, South Korea, China, Australia, and New Zealand. Membership of the AOV is comprised of IVS member organisations and IVS associate members in the Asia-Oceania region. The current member organisations are listed in Table 1.

The AOV organises regular working meetings to improve communication and cooperation between the members. AOV meetings have been held six times since 2015 (see Table 2), in which representatives from member organisations discuss the current status and future direction of AOV activities, including the observing plan and strategies for international collaboration. Information about the AOV, including details and minutes of previous meetings can be found on the AOV website (https://www.spacegeodesy.go.jp/vlbi/AOV/).

Institution	**Country**
Auckland University of Technology	New Zealand
Commonwealth Scientific and Industrial Research Organisation	Australia
Geoscience Australia	Australia
Geospatial Information Authority of Japan	Japan
Korea Astronomy and Space Science Institute	South Korea
National Astronomical Observatory of Japan	Japan
National Geographic Information Institute	South Korea
National Institute of Information and Communications Technology	Japan
National Institute of Polar Research	Japan
Shanghai Astronomical Observatory	China
University of Tasmania	Australia

Xinjiang Astronomical Observatory	China
Corresponding Member Organisations	
Japan Aerospace Exploration Agency (JAXA)	Japan
Space Operations New Zealand	New Zealand
Land Information New Zealand (LINZ)	New Zealand

Table 1. Member organisations of the AOV (as of August 2026). Transferring the membership registration from Auckland University of Technology to Land Information New Zealand is currently underway.

Meeting	**Date**	**Venue**
1st AOV Science and Technology Meeting	November 19-20, 2015	Hobart, Australia
2nd General Meeting of the AOV	July 31 - August 1, 2017	Kobe, Japan
3rd Meeting of the AOV	November 9-10, 2018	Canberra, Australia
4th Meeting of the AOV	September 28, 2022	online
5th Meeting of the AOV	March 7, 2024	Tsukuba, Japan
6th Meeting of the AOV	November 26, 2025	online

Table 2. Past meetings of the AOV.

2.2 Network Stations

A map of the AOV network stations is shown in Figure 1. Due to the geographical characteristics of the Asia–Oceania region, the network extends predominantly in the north–south direction on a global scale, while its longitudinal extent remains relatively limited. The AOV network spans approximately 88◦ in longitude. Ignoring the SYOWA station in Antarctica which only joins occasionally, this was calculated between the most eastern station in New Zealand (WARK12M) and the western edge of the network in URUMQI. This limited geometry constitutes one of the distinctive features of the AOV network among existing VLBI networks. The sensitivity of VLBI observations to EOP

115 strongly depends on network geometry. In general (as for example discussed in Schartner,
116 et al. 2020), long east-west baselines provide high sensitivity to dUT1, whereas north–
117 south baselines are particularly sensitive to the X and Y components in polar motion. Yet,
118 common visibility between participating stations is also critical. Accordingly, the AOV
119 network is expected to be sensitive to polar motion, while being comparatively less
120 sensitive to measuring dUT1.
121 Another characteristic of the AOV network is the concentration of stations in the mid-
122 latitude regions of the northern and southern hemispheres, reflecting the geographical
123 distribution of the participating countries, Japan, China, South Korea, Australia, and New
124 Zealand. In the future, participation of additional stations in equatorial regions, such as
125 Thailand and Indonesia, is anticipated to improve the spatial coverage of the network by
126 filling the current geographical gaps. Simulations about this scenario are discussed in
127 Section 5.
128 In Figure 2, the observing history of stations is shown. During the whole period in which
129 AOV sessions have been conducted, the participating stations in the observations
130 gradually changed over time. This is predominantly due to the IVS' transition from the
131 legacy S/X system to the VLBI Global observing system (VGOS, Petrachenko et al. 2009;
132 Niell et al. 2018). While several legacy S/X stations terminated their operations, new
133 stations have recently expressed their intention to participate in AOV sessions. As a result,
134 despite the composition of participating stations varying from session to session, the AOV
135 sessions have overall maintained a stable number of network stations. On average, 7 to 8
136 stations participate in each session. From 2020, mixed-mode correlation has started for
137 AOV sessions, which enables VGOS stations to participate in AOV legacy S/X sessions
138 with a VGOS receiver (McCallum et al. 2022). Details of the mixed-mode correlation are

described in Section 3.

2.3 Session types

AOV sessions are observed with legacy S/X mode. The sessions are planned through the IVS master schedule (https://ivscc.gsfc.nasa.gov/sessions/yyyy/), in coordination with the IVS Coordination Centre. This allows for operational file distribution (i.e. schedules and station logs), as well as archival and public access of data products via IVS data centres.

Scheduling and correlation are shared among three AOV member organisations: University of Tasmania (UTAS), Geospatial Information Authority of Japan (GSI), and Shanghai Astronomical Observatory (SHAO). For each session, one of these organisations is responsible for scheduling or correlation, and in many cases, the same organisation performs both tasks. The objectives and observing strategies of the session depend largely on the responsible scheduler. UTAS primarily prepares schedules for geodetic and R&D objectives. Similarly, GSI conducts sessions for geodetic objectives, while also especially aiming to determine the positions of Japanese stations such as SYOWA, VERAMZSW, UCHINOUR and USUDA64. By contrast, sessions scheduled by SHAO focus on determining the station coordinates of KUNMING and TIANMA65, as well as on densifying the source catalog for spacecraft tracking in certain regions of the sky. For the remainder of this paper, the discussion mainly focuses on the geodetic results obtained from these sessions.

3. Methods

3.1 Observing mode

In geodetic VLBI (e.g., Nothnagel 2025; Sovers et al. 1998), the measurement precision σ of an individual observation predominantly depends on the amount of signal received by the telescope pair, the signal-to-noise-ratio (SNR), and the recording bandwidth B (Eq. 1).

$$\sigma = \pm \frac{1}{2\pi} \cdot \frac{1}{SNR \cdot B} \quad (1)$$

Additionally, observations are performed in two frequency bands, in the X-band around 8.4 GHz and in the S-band around 2.2 GHz, allowing to correct for effects caused by the ionosphere. In order to achieve recording bandwidths beyond the technical feasible limits of samplers and recorders, VLBI routinely makes use of the bandwidth synthesis technique. As described by Rogers (1970), the key-characteristic of a large bandwidth can also be achieved by only observing a certain set of sub-bands. Information about the exact frequencies and the number and width of the individual channels is captured in the observing mode. When setting the observing mode, the capabilities of each individual telescope has to be taken into account. In VLBI, an observation is formed between a pair of telescopes observing the same target at the same time, using the identical observing mode. In today's legacy S/X VLBI, typically 10 channels are observed in X-band and 6 channels in S-band. The channel bandwidth ranges from 4 MHz to 16 MHz. Considering all channels in both bands, as well as the sampling bit rate, recording data rates of a total of 128 Mbps (Mega-bit per second), 256 Mbps or 512 Mbps are in use. This data rate is important when planning the VLBI sessions. For the scheduling, an estimate about the scan duration tscan needs to be known prior to the observations. The target precision defines a target SNR for each observation, which can then be used to calculate the scan duration. For up to 2-bit sampling, the following relation holds:

$$t_{scan} \propto \left(\frac{SNR}{F}\right)^2 \cdot \frac{SEFD_1 \cdot SEFD_2}{\text{data rate}} \quad (2)$$

Hereby, F is the observed source flux density and SEFD is the source equivalent flux density, characterising the sensitivity of the participating telescopes. According to Eq. 2, a higher data rate allows for a shorter scan duration, which, if applied smartly during the scheduling process, should allow for more observations in one session and ultimately better results. This concept is also one of the underlying ideas behind VGOS, namely that a higher recording rate enables more observations which then will be used to beat the dominating error source due to the atmosphere (e.g., Petrachenko et al. 2009; Pany et al. 2010). It was further practically shown in the AUSTRAL campaign (Plank et al. 2016). The AUSTRAL sessions are legacy S/X sessions using a recording rate of 1 Gbps, which is higher than in common IVS sessions. It could be shown that the observations using a higher data rate and smarter scheduling delivered improved results.

For the AOV sessions, three new observing modes were developed (Table 3). Mode AOVSX4N was used when the stations in SYOWA and VERAMZSW participated (e.g. AOV011). These stations (at that time) had limited recording bandwidth and frequency range. This mode has a total recording rate of only 128 Mbps, using 4 MHz wide channels. AOV16SXN (e.g. AOV010) is another narrow-band mode, tuned for capabilities of the Japanese recording system at stations KASHIM11 and KOGANEI. These stations were able to adopt a 1 Gbps recording, yet with a limited bandwidth in X-band. AOVSX16W (e.g. AOV006) has the same covered bandwidth in X-band as common IVS S/X observations but using 16 MHz channels achieves a 1 Gbps recording rate. The bandwidth in S-band was restricted, in order to avoid unwanted radio frequency emissions at some of the stations. Using simulations, McCallum et al. (2019) showed that by using a higher recording mode than in standard legacy S/X sessions by the IVS, improved results in

terms of baseline lengths repeatabilities can be expected for the AOV sessions.

While these were the three initial modes, during the course of 100 AOV sessions slight modifications of the modes above were also used. This is a result of technical changes and improved capabilities at the stations, as well as an effect of various staff changes responsible for creating the schedules at the different institutions.

Ensuring mode-compatibility across a VLBI network is at the core of this technique. The work described here contributed significantly to initially share this knowledge among members of the AOV and subsequently making sure that this expertise is kept and passed on to new colleagues.

AOVSX4N	128 Mbps	**AOVSX16N**	1 Gbps	**AOVSX16W**	1 Gbps
freq. (MHz)	bw (MHz)	freq. (MHz)	bw (MHz)	freq. (MHz)	bw (MHz)
8208.99	4	8213.99	16	8213.99	16
8218.99	4	8233.99	16	8253.99	16
8248.99	4	8253.99	16	8353.99	16
8308.99	4	8333.99	16	8513.99	16
8418.99	4	8413.99	16	8733.99	16
8498.99	4	8513.99	16	8853.99	16
8548.99	4	8533.99	16	8913.99	16
8568.99	4	8573.99	16	8933.99	16
2213.99	4	2223.99	16	2223.99	16
2228.99	4	2243.99	16	2243.99	16
2238.99	4	2263.99	16	2263.99	16
2268.99	4	2293.99	16	2293.99	16
2288.99	4	2343.99	16	2343.99	16
2293.99	4	2363.99	16	2363.99	16

Table 3. Initial observing modes for AOV sessions. Most AOV sessions are observed with 1 Gbps recording, which is higher than in the IVS legacy S/X sessions.

3.2 Scheduling

As mentioned Section 2, AOV sessions are governed by three scheduling strategies implemented by UTAS, GSI, and SHAO.

In UTAS, scheduling expertise was first gained through the AUSTRAL observing campaigns (Plank et al. 2016). After those very regional sessions, AOV sessions provided the next step up. The geographical situation as well as a very diverse network in telescope sensitivity and slew speeds regularly require manual iterative optimisation of the scheduling process. A high priority is put on the criterion that all telescopes are scheduled for a sufficient number of observations and do not have significant idle times. We also regularly adapt the weighting in the scheduling, in order to aim for larger scans comprising of the (almost) full network, rather than splitting the network in two sub-nets (north and south), which is often preferred by the scheduling algorithm due to the fact that it overall allows for more observations. In the beginning, VieVS (Sun et al. 2014) was used at UTAS for scheduling the AOV sessions. Since 2023, VieSched++ (Schartner and Böhm 2019) is used.

In GSI, schedules are currently generated using the scheduling software program VieSched++. Before AOV094 in 2024, the software SKED (Gipson 2016) was used instead of VieSched++. The fundamental strategy in the scheduling by GSI is to ensure that the station positions of the participating local stations are determined with high accuracy. For its purpose, the integrated simulator of VieSched++ is used to ensure that the created schedule is optimized for the local stations. In particular, when SYOWA station in Antarctica participates, the limited observing opportunities and the high importance of AOV sessions for the station necessitates assigning a greater weight to

SYOWA in the scheduling process. USUDA64 is tagged-along in the session when participating in, given its slow slewing speed of 0.25 deg/s along AZ and EL directions. Because neither UTAS nor GSI routinely schedules global IVS sessions other than AOV, as well as the need for specific AOV observing modes (see Section 3.1), the schedules are typically sent out to the stations a week prior to the session date. This allows for potential errors in the schedule files to be captured and corrected in time.

In SHAO, all schedules were made using the SKED software, based on the early scheduling expertise gained from Chinese domestic geodetic observing program. Because Chinese VLBI stations are frequently involved in spacecraft tracking and the relevant plans are often notified at short notice, AOV schedules are generated in a more real-time manner, typically 3–5 days before the observation date, to reduce the impact of station unavailability. To achieve higher sensitivity, all sessions were scheduled at a 1 Gbps data rate, first introduced in AOV004, so as to better balance geodetic and astrometric objectives. In addition to regularly used geodetic sources, which are typically strong and compact, a list of selected astrometric sources was also specified for scheduling in many cases. Although the automatic mode in SKED was used, manual iterative optimization was still necessary, similar to the approach adopted by the other two institutes. If TIANMA65 is included, its limit of a maximum of 12 scans per hour requires the configuration parameters to be adjusted accordingly.

3.3 Correlation

Correlation of AOV data is also shared among UTAS, GSI and SHAO. While SHAO regularly takes on correlating global IVS sessions, the AOV sessions are the largest sessions for UTAS and GSI to work with. Besides the logistical work of data transport,

sufficient data storage and processing capabilities need to be in place. Even more important, the expert knowledge and workforce required for geodetic VLBI fringe fitting and post processing cannot be emphasized enough.

One of the key features of more recent AOV sessions is that the correlation is processed in a mixed-mode, handling observational data of both S/X and VGOS stations. The following subsection describes the development of mixed-mode observation and correlation in AOV sessions.

3.4 Mixed-mode observation and correlation

The mixed mode observing is a practical solution to a significant issue emerging from the transition of IVS observations from legacy S/X systems to VGOS. This issue was particularly prevalent in the AOV region.

Japan was one of the fastest countries in adopting VGOS, also having detailed plans for managing the transition. In Japan, a new VGOS telescope was built in Ishioka, starting IVS observations in 2015. At that time, VGOS observing within the IVS had not progressed to an operational stage yet. The long-serving Japanese IVS station TSUKUB32 was demolished at the end of 2016. This caused the situation that there was no Japanese station left in the core IVS sessions, which were still observed in legacy S/X mode. As an initial solution, Ishioka station was swapping receivers several times per year, participating in legacy S/X observations for half of the year and in VGOS sessions for the remainder. Each receiver change required several weeks of downtime for the station and a significant amount of human resources. Even more critical was the situation with the Australian stations. The AuScope VLBI array (Lovell et al. 2013) is one of the most active networks participating in the operational IVS sessions, making up a large

294 portion of southern hemisphere stations in the IVS network. Since these telescopes were
295 already originally designed with VGOS in mind, between 2017 and 2023 all three
296 telescopes were upgraded with VGOS receivers and back-ends. As a consequence, one
297 by one the Australian telescopes disappeared from the IVS legacy S/X sessions, leaving
298 a significant gap in the global VLBI network.
299 As a solution, the Australian mixed-mode was developed. As described in detail in
300 McCallum and McCallum (2019) and McCallum et al. (2022), this technique allows the
301 VGOS stations to record in legacy S/X mode, thus joining the IVS network still used for
302 the majority of VLBI products. This is by overcoming significant differences between the
303 two systems, as described in Table 4.
304 The operational VGOS observing starts at 3+ GHz. While some of the used feed horns
305 have sensitivity below that, physical filters often block out signals in the legacy S-band
306 frequency span in order to prevent unwanted electromagnetic radiation entering the signal
307 chain. By default, a VGOS station is not capable to receive the legacy S-band signal. The
308 other big difference is the polarisation. While in legacy S/X the receivers are circularly
309 polarised, typically using the right hand circular signal, in VGOS two linear polarisations
310 are recorded. And lastly, with VGOS bringing recording capabilities to a new level,
311 sometimes the used samplers/recorders are not well suited to record smaller bandwidths.
312 In brief, the mixed-mode technique overcomes these issues as follows:
313 (1) At mixed-mode stations, the S-band signal is preserved, e.g., by bypassing the
314 bandpass filter and transporting the signal in a separate (spare) data cable. As common in
315 legacy S/X VLBI, it still may be mixed and down-converted and transported via a coaxial
316 cable instead of the fibre used in VGOS.
317 (2) Both data streams (two linear polarisations) are recorded. They are quasi-converted

into a circular product during fringe fitting and post processing after the correlation process, requiring special consideration of all cross-polarisation products.

(3) Certain restrictions in the samplers and recording format prevent the mixed mode stations recording the two lower side-bands of the legacy X-band. Some stations also prefer to record 32 MHz channels instead of 16 MHz, in order to avoid performance loss at band edges.

(4) It could be shown that certain VGOS stations can successfully mimic a legacy S/X recording, as long as some extra steps are taken during correlation and fringe fitting and also accepting the fact that mixed-mode stations have to record about twice as much data as standard legacy S/X stations.

Having tested the mixed-mode technique in the AUSTRAL sessions, it was applied to AOV sessions next. These international sessions, together with the fact that mixed-mode removed the need for Ishioka to swap receiving systems helped for this technique to be accepted by the international IVS community. Today, five key stations in Australia, Japan and Norway are regularly using mixed-mode, helping maintain a sustainable global network for the routine IVS legacy S/X observations until VGOS will be operating fully with multiple sessions per week.

	VGOS	**legacy S/X**
Frequency:	3-14 GHz	S- & X-band (2.2 & 8.4 GHz)
Polarisation:	two linear polarisations	rcp (right-hand circular)
Recording:	large channels of 16 or 32 MHz	4-16 MHz channels

Table 4. Differences between VGOS and the legacy S/X observing.

3.5 Analysis

Routine analyses of AOV sessions are conducted by the NASA/GSFC analysis centre, and their results are submitted to the IVS. For this study, all past AOV sessions were reanalysed collectively using CALC/SOLVE (Ma et al. 1990).

In the analysis, observational database vgosDb files comprising 100 AOV sessions from AOV001 observed on March 21 in 2015 to AOV100 on August in 2025 were processed together with other 2314 IVS sessions observed in the same time period as AOV001–AOV100. The estimated parameters include the station positions, source positions, EOP, zenith atmospheric delays (20 minutes intervals), clock variations (60 minutes intervals), and atmospheric gradients (6 hours intervals). A-priori values for station positions are created from ITRF2020-u2024 (Altamimi et al. 2023) with modifications for local stations along with post-seismic deformation (PSD) models. Radio source positions are constrained to ICRF3 (Charlot et al. 2020) as a priori values. No-Net Rotation (NNR) and No-Net Translation (NNT) constraints are applied to stations positions, and NNR constraints are applied to source positions in the analysis. If a session has fewer than 8 observations of a station, 4 observations of a source, or 3 observations of a baseline, these observations are excluded from the analysis. All analysis conditions were described in a control file, and the analysis was carried out following the CALC process to compute time delays and delay rates, and the OPA (Operational Analysis utility) process to update arc files and weight files.

4. Results

4.1 EOPs

Figures 3, 4 and 5 present uncertainties in dUT1, X polar motion, and Y polar motion, respectively, for each AOV session derived from the analysis in Section 3.5. For

363 comparison, other types of IVS global and regional sessions were analysed in the same
364 manner, and their results are overlaid in the figures. The four session types compared in
365 this study are IVS-R1, IVS-R4, AUSTRAL, EUROPE and OHIGGINS sessions. The
366 IVS-R1 and R4 sessions are conducted weekly to provide EOP results submitted to the
367 IERS on a timely basis (Thomas et al. 2024). The network consists of 8 to 14 stations
368 distributed globally, including several AOV stations: HOBART12, KATH12M,
369 YARRA12M, WARK12M, and SEJONG for the R1 and R4 sessions, with ISHIOKA
370 additionally participating in the R1 sessions.
371 The other three types are regional IVS sessions. OHIGGINS sessions have the largest
372 network size out of those three session types, consisting of OHIGGINS, SYOWA, AGGO,
373 FORTLEZA, HART15M, HOBART26, WARK12M, TIGO as well as KOKEE, to tie
374 together optimally the sites in the Southern Hemisphere, including VLBI telescopes in
375 Antarctica. AUSTRAL sessions also comprise a Southern Hemisphere network,
376 including HOBART12, KATH12M, YARRA12M, WARK12M and HART15M (Plank
377 et al. 2016). EUROPE sessions are experimental for the purpose of determining the station
378 coordinates and their evolution in the European geodetic VLBI network.
379 As shown in Figure 3 and Table 5, the AOV sessions exhibit the largest uncertainty in
380 dUT1, 36.29 μs in median values. The R1 and R4 sessions yield the smallest uncertainties,
381 17.84 μs and 15.48 μs respectively, in median values in the period after March 2015,
382 while the AUSTRAL, OHIGGINS, and EUROPE sessions show intermediate values. The
383 result is considered to reflect the geometric characteristics of the observing network for
384 each session type. The east-west baseline length of the AOV network extends to 6951 km
385 between SYOWA and WARK12M stations. Given that SYOWA station participates in
386 AOV sessions only once per year, it is evident that AOV sessions are fundamentally

conducted with a network configuration that is short in the east-west direction and consequently rather insensitive to measuring dUT1. In fact, when the 13 AOV sessions including SYOWA station are selected, the median of the uncertainty of dUT1 is 24.60 μs, demonstrating a sensitivity comparable to that of other regional sessions.

On the other hand, the uncertainties in X and Y polar motion derived from AOV sessions are comparable to those of other regional sessions as shown in Figure 4, 5 and Table 5, indicating that similarly high accuracy was achieved. Among all sessions examined, the global R1 session yielded the lowest formal errors, with median uncertainties of 204.4 μas and 245.8 μas for the X-pole and Y-pole, respectively. In contrast, the AUSTRAL sessions and EUROPE sessions exhibit largest uncertainties in the X-pole and Y-pole components, respectively. This suggests that the geometrical distribution of participating stations in these sessions results in reduced sensitivity to measuring polar motion. It should be noted that AOV and the other regional sessions are primarily intended to determine station coordinates within their respective regions, and unlike the R1 sessions, the rapid determination of EOP is not their primary objective. The following subsection presents the station coordinates obtained from AOV sessions.

Session	**dUT1 [μs]**			**X-pole [μas]**			**Y-pole [μas]**		
	25%	50%	75%	25%	50%	75%	25%	50%	75%
AOV	26.57	36.29	48.47	154.54	204.40	342.31	155.11	245.75	363.40
R1	16.55	17.84	19.60	36.66	50.70	77.55	44.31	62.42	93.79
R4	14.31	15.48	16.96	48.15	63.72	95.87	55.69	79.13	112.20
AUSTRAL	23.08	27.30	38.63	272.39	363.85	524.74	211.25	314.68	543.37
OHIGGINS	23.45	25.06	28.19	222.77	278.87	369.75	210.11	254.77	297.31
EUROPE	21.20	23.85	28.74	208.64	312.02	384.69	315.01	412.13	523.04

Table 5. First quantile, median and third quantile for formal uncertainties of EOPs from each type of sessions. Median values are presented with lines in Figure 3, 4 and 5.

4.2 Station coordinates

Figure 6 presents the time series of station coordinates in the X, Y, and Z directions for the ISHIOKA, YARRA12M, and URUMQI stations as examples, among those obtained from the AOV sessions. For comparison, station positions derived from other sessions are also overlaid in the figure. ISHIOKA station is affected by post-seismic deformation associated with the 2011 Tohoku earthquake, exhibiting notable nonlinear components particularly in the velocities of the X and Y directions. Figure 7 compares the uncertainties in the X, Y, and Z positions obtained from AOV sessions and other IVS sessions combined for each station. The results from the AOV sessions are consistent with those from other sessions, and the magnitude of the uncertainties is comparable to that of the other session types. A comparison of the uncertainties indicates that SESHAN25 and TSUKUB32 exhibit particularly high precision. Although many VGOS stations participate in the AOV sessions, the observing frequency setup is S/X mode in current AOV sessions. Therefore, stations with larger antenna diameters and relatively high slew speeds demonstrate the best performance under these conditions. Meanwhile, VGOS stations such as HOBART12, ISHIOKA, KATH12M and YARRA12M also achieve sufficiently high precision, well below the 1 cm level.

Table 6 lists the total number of IVS sessions included in this analysis as well as the number of AOV sessions for each station. In particular, the proportion of AOV sessions relative to the total number of sessions since 2015 exceeds 20% for AIRA, KOGANEI, KUNMING, SYOWA, TIANMA65, URUMQI, USUDA64 and VERAMZSW stations,

indicating that AOV sessions make a substantial contribution to station position determination in recent years at these sites. Among these stations, KUNMING, SYOWA, TIANMA65 and VERAMZSW showed particularly large improvements in precision as a result of the AOV sessions, as illustrated in Figure 7.

Station	AOV sessions	IVS sessions	Ratio of AOV in IVS
AIRA	1	1	100%
HOBART12	49	699	7%
HOBART26	32	342	9%
ISHIOKA	73	653	11%
KASHIM11	11	72	15%
KASHIM34	10	55	18%
KATH12M	70	996	7%
KOGANEI	42	110	38%
KUNMING	49	106	46%
SEJONG	49	508	10%
PARKES	1	10	10%
SESHAN25	42	215	20%
SYOWA	16	77	21%
TIANMA65	15	35	43%
TSUKUB32	12	120	10%
URUMQI	46	111	41%
USUDA64	2	2	100%
VERAMZSW	30	60	50%
WARK12M	76	687	11%
YARRA12M	86	1317	7%

Table 6. Total number of IVS sessions and AOV sessions used in this analysis for each station. UCHINOUR station is excluded in this table because it has only participated in AOV100 session but is not used in this analysis.

4.3 Baseline length repeatabilities

The impact of the AOV sessions is further proven by studying baseline lengths repeatabilities. For the analysed sessions, we derive baseline length repeatabilities as the weighted root mean square (WRMS) of the estimated baseline length between two stations for each session ($\widehat{bl}_i$) minus the a priori length ($\widetilde{bl}_i$) given by the ITRF for that time (Eq. 3).

$$WRMS = \sqrt{\frac{\sum_{i=1}^{n} \frac{\widehat{bl}_i - \widetilde{bl}_i}{\sigma_i^2}}{\sum_{i=1}^{n} \frac{1}{\sigma_i^2}}} \tag{3}$$

For weights, we use basic error-propagation applied to the station-wise formal errors (ϵ) as calculated for each session (Eq. 4).

$$w_i = \sqrt{\frac{(\epsilon_{x1} - \epsilon_{x2})^2 + (\epsilon_{y1} - \epsilon_{y2})^2 + (\epsilon_{z1} - \epsilon_{z2})^2}{3}};\ \sigma_i = \frac{1}{w_i} \tag{4}$$

In Figure 8, baseline length repeatabilities are shown for the AOV sessions, the R1 sessions and all analysed session.

Overall we find repeatabilities of a few millimetres for short baselines, 1-2 cm for the mid-range and up to 3 cm or more for long baselines. This is in line with the results from other IVS sessions. The two outliers in the results are the baseline SEJONG–SYOWA at 189 mm wrms and HOBART26–TIANMA65 at 56 mm wrms.

Studying the differences in the results between AOV sessions and all IVS sessions (as shown with the black bars in Figure 8), we find that from the 61 overlapping baseline pairs, 24 are worse in the AOV sessions and 36 are better determined in the AOV sessions having lower wrms. Baseline WARK12M–TIANMA65 was exclusively observed in 13 AOV sessions with a precision of 37 mm wrms. As shown in Figure 8, linear fits to the AOV sessions (y = 2.32x [mm / 1000 km]) and all IVS sessions (y = 2.55x [mm / 1000

km]) further confirm that the AOV sessions tend to exhibit slightly lower WRMS values than the overall IVS sessions.

Table 7 shows the baselines where the difference between the precision of AOV sessions and all sessions is larger than 5 mm. For the stations VERAMZSW and SEJONG, the AOV sessions show significant positive impact. This result indicates that, as discussed in Sections 3.2 and 4.2, one of the primary objectives of AOV sessions is to ensure high station position accuracy for local stations in the Asia-Oceania region. Improvements observed in baseline length repeatability for these stations further demonstrate the effectiveness of AOV sessions in achieving this objective.

Baseline	**WRMS AOV (sess.)**	**WRMS all (sess.)**	**+/−**
HOBART26–KOGANEI	16.3 (13)	21.5 (29)	+
HOBART26–SEJONG	11.2 (10)	28.2 (52)	+
HOBART26–YARRA12M	13.7 (31)	7.7 (215)	−
ISHIOKA–SYOWA	20.0 (11)	29.1 (14)	+
KATH12M–WARK12M	19.3 (52)	8.8 (437)	−
KATH12M–YARRA12M	9.3 (61)	15.7 (825)	+
SEJONG–VERAMZSW	4.2 (20)	15.8 (46)	+
SEJONG–WARK12M	18.5 (38)	30.7 (143)	+
SYOWA–YARRA12M	24.4 (15)	18.0 (62)	−
VERAMZSW–WARK12M	12.4 (25)	17.6 (28)	+
VERAMZSW–YARRA12M	15.6 (27)	20.8 (43)	+
WARK12M–YARRA12M	12.6 (66)	2.9 (565)	−

Table 7. Baseline length repeatabilities (wrms) in mm for the analysed sessions, comparing results for all sessions and AOV sessions. A plus (+) in the last column indicates that the precision of the AOV sessions is better than compared to all IVS sessions.

5. Beyond AOV100: Future Prospects of AOV sessions

5.1 Potential contribution of new stations in Thailand and Indonesia to the AOV network

The IVS VLBI network has been steadily expanding in recent years. As noted above, the development of VLBI antennas is also progressing in the Asia–Oceania region, with new stations expected to participate in AOV observations. In Thailand, National Astronomical Research Institute of Thailand (NARIT) is currently advancing the operation of a VGOS antenna in Chiang Mai (Shang-Guan et al. 2025), actively testing with other stations such as the Shanghai Astronomical Observatory. In addition, in Bandung, Indonesia, a VGOS antenna has been constructed at Bosscha Observatory in Bandung Institution of Technology (ITB), and preparations for regular observations are underway (Ramadhan et al. 2024).

In this section, a simple simulation was performed to evaluate the extent to which the accuracy of AOV sessions may improve when these new stations join the AOV network. The software employed in this simulation is VieSched++, which is used for scheduling of regular AOV sessions. The target sessions are AOV098 conducted on March 19, 2025, and AOV100 conducted on August 14, 2025, which are the two most recent sessions among the 100 sessions scheduled by GSI. New stations in Thailand (hereafter referred to as CHIANG13) and Indonesia (BOSSCHA) were added to these sessions, and the resulting EOP accuracies were compared with those simulations obtained from the original schedules, AOV098 and AOV100. The specifications assumed for CHIANG13 and BOSSCHA in this study are summarized in Table 8. Parameters for CHIANG13 were basically taken from Shang-Guan et al. (2025), and for parameters not publicly available, values were adopted based on information obtained from private communication with

station personnel and confirmed to be consistent with those of typical VGOS antennas. SEFD is calculated by the following equation:

$$SEFD = \frac{2k_B T_{sys}}{A_e}, \quad (5)$$

where k_B is the Boltzmann constant, A_e is the effective area and T_{sys} is the system temperature, which is typically ~40 K for CHIANG13 and BOSSCHA stations.

The simulations are performed for different combinations of weight factors assigned to sky coverage, the number of observations, scan duration, and idle time. For each combination, 1,000 simulations are carried out to evaluate the repeatability of the EOPs. A white noise level of 17.68 ps, corresponding to a typical S/X VLBI observation, an Allan Standard Deviation of 10−14 for the clocks, and a homogeneous refractive index structure constant (Cn = 1.8×10−7 m−1/3) model are adopted throughout the simulations (Schartner and Böhm 2020; Schartner 2025).

The simulation results are shown in Figure 9. Both in AOV098 and AOV100, the expanded network including CHIANG13 and BOSSCHA resulted in accuracy improvements of a few percent to a maximum of 20% for all estimated parameters, polar motion X, polar motion Y, and dUT1. The addition of these two new stations effectively fills the geographical gap between the Northern and Southern Hemispheres, thereby strengthening the observational network. As a result, this enhancement is considered to contribute to the improved repeatability of the EOP estimates. It should be noted that the repeatability discussed in this section is derived from simulations using VieSched++, and therefore cannot be directly compared with the uncertainties obtained from the analysis of actual observations discussed in Section 4, as the underlying assumptions differ between the two approaches such as the estimated parameters. Another important factor to be considered is the potential degradation of the SNR in actual observations due to

radio frequency interference (RFI). The S band in S/X observations is particularly vulnerable to RFI, and stations operating in unfavorable radio-frequency environments may require extensive filtering of affected frequency channels. Investigations of the RFI conditions at ChiangMai and Bosscha stations are currently in progress. Consequently, future observational campaigns will require appropriate tuning of the frequency configuration and related observing parameters in accordance with the RFI environment at each station.

	CHIANG13	**BOSSCHA**
Position X [m]	−967208.00	−1916855.70
Position Y [m]	5960005.00	6036257.85
Position Z [m]	2049428.00	−752925.70
Dish Diameter [m]	13.0	13.0
Slew Rate Az [deg / s]	12	12
Slew Rate El [deg / s]	6	6
SEFD S-band [Jy]	1500	1500
SEFD X-band [Jy]	1500	1500

Table 8. Antenna specifications for CHIANG13 and BOSSCHA used in the simulation.

5.2 AOV VGOS Sessions

All AOV sessions to date have been conducted with legacy S/X setup, and no official VGOS observations have been carried out by AOV. As the number of VGOS antennas within the AOV network has been increasing, and as correlators have accumulated experience in processing VGOS sessions through IVS activities, AOV has been preparing for conducting VGOS observations in recent years.

To examine the feasibility of conducting AOV VGOS observations, an experimental one-hour VGOS session (VAO001) was carried out in May 2025. Seven stations, HOBART12,

ISHIOKA, KATH12M, SESHAN13, TIANMA13, URUMQI13, and YARRA12M participated in the session. The observational data were correlated and analysed independently by UTAS, GSI, and SHAO, and a comparison of the results is currently in progress.

Furthermore, an experimental 24-hour VGOS session (VAO002) was observed in July 2026, with ISHIOKA, SESHAN13, and KATH12M. With the limited available network the goal of this session was not geodetic results, rather it was to assess current operational VGOS scheduling, logistics and correlation capabilities within the AOV group. This session was successfully correlated and post-processed according to IVS standard VGOS procedures.

The success of VAO002 has prompted the further planning of more VAO sessions, with the aim of moving these sessions to the official IVS calendar to ensure the persistence of all geodetic products. While VAO sessions are the natural path forward for the future of AOV VLBI, we also envisage these sessions playing a critical role in assisting upcoming VGOS stations in achieving operational capabilities. These sessions will provide a testbed for assessing station performance and troubleshooting problems as these stations work towards participating in operational IVS VGOS sessions.

We conducted similar simulations as in Section 5.1 to evaluate geodetic parameter estimation for VGOS sessions. A test session VAO999, was scheduled using VieSched++. The station network consisted of 7 stations, HOBART12, ISHIOKA, KATH12M, SESHAN13, TIANMA13, URUMQI13, and YARRA12M. The schedule was made using fixed scan durations of 30 seconds, with most scans being scheduled for the entire network. This results in about 60 scans per hour per station. For the VGOS simulations, a white-noise level of 2.83 ps was assumed (McCarthy et al. 2025), while all other settings

were identical to those described in Section 5.1.

The results are shown in Figure 10. For VAO999, a substantial improvement in station position repeatability is observed at all comparable VGOS stations relative to AOV098 and AOV100, with values decreasing from approximately 5 mm to 3 mm. This demonstrates that VGOS observation are expected to achieve higher station position precision than conventional legacy S/X observations, owing to their wider observing bandwidth and faster antenna slewing capabilities.

In contrast, there is no improvement for VGOS in terms of EOP. The repeatability of the EOP estimates is comparable between AOV098 and VAO999. This can be attributed to a trade-off between the intrinsic advantages of VGOS observations and the more limited geographical extent of the current AOV VGOS network compared to the S/X network. In particular, the AOV VGOS network still lacks sufficiently long east-west baselines for accurate determination of dUT1, which likely offsets the performance gains expected from the VGOS observing system. To achieve more precise EOP estimates from AOV VGOS observations, participation of additional VGOS stations distributed over a wider geographical area, will be desirable in the future.

6. Conclusions

In this paper, we analysed 100 sessions conducted by the AOV network and statistically compared the results with those obtained from other observing sessions in the IVS. Among the estimated EOPs, the accuracy of dUT1 was generally lower than that achieved by other sessions, primarily due to limitations in the AOV network geometry. In contrast, the accuracies of the polar motion estimates were comparable to, or better than, those obtained from other sessions. For station position estimates, all stations showed results

588 consistent with those from other sessions and achieved comparable repeatability.
589 Specifically for stations that are not regularly participating in IVS observations, the
590 results from the AOV sessions was found to have impact. The AOV observations provide
591 a crucial connection between the global VLBI network and the regional networks in the
592 Asia–Oceania region. Consequently, they serve as a bridge between the ITRF and
593 national and regional geodetic reference frames, thereby contributing substantially to the
594 consistency of these reference frames.
595 As a future prospect for AOV activities, we assessed the expected impact of incorporating
596 two new stations in Thailand and Indonesia into the current AOV observing network. The
597 addition of these stations was predicted to improve the accuracy of all EOP parameters
598 by several percent to approximately 20% relative to the existing network configuration.
599 Furthermore, future plans for AOV VGOS observations were presented, together with
600 simulations of the expected performance, indicating continued growth and increasing
601 activity within the AOV framework.
602 The success of VLBI observations depends on the establishment and cooperative
603 operation of a well-balanced global VLBI network. The Asia-Oceania regional network
604 has been gradually strengthened and expanded, enabling stable AOV observations both
605 in S/X and VGOS. Continued efforts will be made to further enhance geodetic VLBI
606 observations throughout the Asia–Oceania region, accumulate scientific and operational
607 achievements, and foster the sharing of expertise and the transfer of technical knowledge
608 among participating institutes in the AOV.
609

610 **Declarations**

611 **Availability of data and materials**

All AOV and IVS sessions are publicly available through the IVS, at https://ivscc.gsfc.nasa.gov/. The specific datasets and results used during the current study are available from the corresponding author on reasonable request.

Competing interests

The authors have no competing interests to disclose.

Funding

The authors received no dedicated funding for this work.

Authors' contributions

Study conception and design were primarily developed through discussions between Masafumi Ishigaki and Lucia McCallum. These two authors wrote the manuscript. Masafumi Ishigaki investigated the EOPs and station coordinates obtained by AOV and other sessions and simulated the impact of new stations. Lucia McCallum wrote the Sections 2.1, 2.3, 3.1 and 3.4. She calculated the baseline lengths repeatabilites and did the VGOS schedule VAO099. Tiege McCarthy scheduled and correlated VAO002 and wrote about it here. Fengchun Shu provided information about the scheduling process at SHAO. Analyses presented in Section 3.5 were performed by Haruna Furui, Takehiro Nishi and Tetsuya Hara.

Acknowledgements

The AuScope VLBI project is managed by the University of Tasmania, contracted through Geoscience Australia. The VLBI array was established with funds provided by

AuScope and the Australian Government via the National Collaborative Research Infrastructure Strategy (NCRIS): auscope.org.au. We are grateful to Taufiq Hidayat for providing the specification of Bosscha VLBI station. We also thank Shinobu Kurihara for valuable feedback on this work as a former member of AOV.

References

Altamimi Z, Rebischung P, Collilieux X, M´etivier L, Chanard K, ITRF2020: an augmented reference frame refining the modeling of nonlinear station motions, J Geod, 97, 5, doi:10.1007/s00190-023-01738-w, 2023.

Charlot P et al., The third realization of the International Celestial Reference Frame by very long baseline interferometry, Astronomy & Astrophysics, doi:10.1051/0004-6361/202038368, 2020.

Gipson J, Goddard Space Flight Center Sked VLBI Scheduling Software, 2016. https://manualzz.com/doc/48679759/nasa-sked-vlbi-scheduling-software-user-manual. Accessed July 31, 2026.

Ishimoto M, Umei M, Toyoda T, Wakasugi T, Kawabata R, Miyahara B, Numajiri K, Nakagawa M (2017) Tsukuba 32-m VLBI Station, in International VLBI Service for Geodesy and Astrometry 2015+2016 Biennial Report, edited by K. D. Baver, D. Behrend, and K. L. Armstrong, NASA/TP-2017-219021, 2017. https://ivscc-vcc.org/publications/br2015+2016/nstskb.pdf

Kurihara S, Lovell J, Cho J, Gulyaev S, Shu F, Kawabata R (2015) Foundation of the Asia-Oceania VLBI Group for Geodesy and Astrometry. In: Baver KD, Behrend D, Armstrong KL (eds) International VLBI Service for Geodesy and Astrometry 2014 Annual Report, NASA/TP-2015-217532, 2015,

https://ivscc.gsfc.nasa.gov/publications/ar2014/spcl-aov.pdf. Accessed 24 Jun 2026

Lovell JEJ et al., The AuScope geodetic VLBI array, J Geod, 87, 527–538,doi:10.1007/s00190-013-0626-3, 2013.

Ma, C., J. M. Sauber, L. J. Bell, T. A. Clark, D. Gordon, W. E. Himwich, and J. W. Ryan (1990), Measurement of horizontal motions in Alaska using very long baseline interferometry, J. Geophys. Res., 95(B13), 21991–22011, doi:10.1029/JB095iB13p21991.

McCallum L, Wakasugi T, Shu F, Current Activities and Plans of the AOV - Asia-Oceania VLBI Group In: Armstrong KL, Baver KD, Behrend D (eds) IVS 2018 General Meeting Proceedings ”Global Geodesy and the Role of VGOS – Fundamental to Sustainable Development”, NASA/CP-2019-219039, https://ivscc.gsfc.nasa.gov/publications/gm2018/29 mccallum etal.pdf. 2019. Accessed 30 Jul 2026

McCallum J, McCallum L, An S/X Compatible VGOS System for the AuScope Array In: Armstrong KL, Baver KD, Behrend D (eds) IVS 2018 General Meeting Proceedings ”Global Geodesy and the Role of VGOS – Fundamental to Sustainable Development”, NASA/CP-2019-219039, https://ivscc.gsfc.nasa.gov/publications/gm2018/27 mccallum mccallum.pdf. 2019. Accessed 31 Jul 2026

McCallum J, McCallum L, Calv´es G. M, Reid B, Ellingsen S, Dickey J (2020) AuScope VLBI Array and Hobart 26-m Antenna, in International VLBI Service for Geodesy and Astrometry 2017+2018 Biennial Report, edited by K. L. Armstrong, K. D. Baver, and D. Behrend, NASA/TP-2020-219041, 2020. https://ivscc.gsfc.nasa.gov/publications/br2017+2018/nshobart.pdf

McCallum L, Chin Chuan L, Krásná H et al. (2022) The Australian mixed-mode observing program, J Geod 96/10:67, doi:10.1007/s00190-022-01657-2

McCarthy T, McCallum L, Schartner M (2025) Investigating a continental Australian VGOS VLBI intensive for UT1-UTC determination. EPS 77:58. https://doi.org/10.1186/s40623-025-02182-0

Niell A, Barrett J, Burns A et al. (2018) Demonstration of a Broadband Very Long Baseline Interferometer System: A New Instrument for High-Precision Space Geodesy, Radio Science 53/10:1269-1291. doi:10.1029/2018RS006617

Nothnagel A, Artz T, Behrend D Malkin Z (2017) International VLBI Service for Geodesy and Astrometry: Delivering high-quality products and embarking on observations of the next generation. J Geod 91:7:711-721. doi:10.1007/s00190-016-0950-5

Nothnagel, A., Elements of Geodetic and Astrometric Very Long Baseline Interferometry, doi:10.48436/jpxxh-74t10, 2025.

Pany A, Böhm J, MacMillan DS, Schuh H, Nilsson T, Wresnik J, Monte Carlo simulations of the impact of troposphere, clock and measurement errors on the repeatability of VLBI positions, J Geod,85:1,39–50, 2010.

Petrachenko B, Niell A, Behrend D et al. (2009) Progress Report of the IVS VLBI2010 Committee: Design Aspects of the VLBI2010 System In: The dictionary of substances and their effects. NASA/TM-2009-214180. https://ivscc.gsfc.nasa.gov/publications/misc/TM-2009-214180.pdf. Accessed 26 Jun 2026

Plank, L, Lovell, J.E.J, McCallum, J.N, Mayer D, Reynolds C, Quick J, Weston S, Titov O, Shabala S.S, B¨ohm J, Natusch T, Nickola M, Gulyaev S (2016) The AUSTRAL

VLBI observing program. J Geod 91, 803–817 (2017). https://doi.org/10.1007/s00190-016-0949-y

Ramadhan S, Hidayat T, Suryana J, Romadhoni A, Kurniasari M, RFI measurements at Bosscha observatory to prepare a new VGOS station, J. Phys.: Conf. Ser. 2773 012015, doi:10.1088/1742-6596/2773/1/012015, 2024.

Rogers, A. E. E., Very long baseline interferometry with large effective bandwidth for phase-delay measurements. Radio Science, 5(10), 1239–1247. doi:10.1029/RS005i010p01239, (1970).

Schartner M and Böhm J, VieSched++: A New VLBI Scheduling Software for Geodesy and Astrometry, "PASP", 131:084501, doi:10.1088/1538-3873/ab1820, 2019.

Schartner M, Böhm J, Nothnagel A (2020) Optimal antenna locations of the VLBI Global Observing System for the estimation of Earth orientation parameters. EPS 72:87.
doi:10.1186/s40623-020-01214-1

Schlüter, W., Behrend, D. The International VLBI Service for Geodesy and Astrometry (IVS): current capabilities and future prospects. J Geod 81, 379–387 (2007). https://doi.org/10.1007/s00190-006-0131-z

Sekido M, Kawai E (2021a) Kashima 11-m and Koganei 11-m VLBI Stations, in International VLBI Service for Geodesy and Astrometry 2019+2020 Biennial Report, edited by D. Behrend, K. L. Armstrong, and K. D. Baver, NASA/TP-20210021389, 2021. https://ivscc.gsfc.nasa.gov/publications/br2019+2020/nsksp.pdf

Sekido M, Kawai E (2021b) NICT Kashima 34-m Report for 2019–2020, in International VLBI Service for Geodesy and Astrometry 2019+2020 Biennial Report, edited by D. Behrend, K. L. Armstrong, and K. D. Baver, NASA/TP-20210021389,

2021. https://ivscc.gsfc.nasa.gov/publications/br2019+2020/nskas.pdf

Shang-Guan, WH., Zhao, RB., Wang, JQ. et al. (2025) Remote health monitoring system for the Chiang Mai 13-m VGOS radio telescope. Exp Astron 60, 8 (2025). https://doi.org/10.1007/s10686-025-10012-0

Schartner M, Böhm J (2020) Optimizing schedules for the VLBI global observing system, J Geod 94, 12 (2020). https://doi.org/10.1007/s00190-019-01340-z

Schartner M (2025) Deriving a global troposphere model for space geodetic simulations based on an ML ensemble featuring uncertainty quantification, J Geod, 99, 72 (2025). https://doi.org/10.1007/s00190-025-01996-w

Sovers OJ, Fanselow, JL, Jacobs, CS, Astrometry and geodesy with radio interferometry: experiments, models, results, Reviews of Modern Physics, 70:4, 1393–1454, 1998.

Sun J, B¨ohm J, Nilsson T, Kr´asn´a H, B¨ohm S, Schuh H, New VLBI2010 scheduling strategies and implications on the terrestrial reference frames, J Geod, 88, 449–461, 2014.

Thomas CC, MacMillan DS, Le Bail K (2024) Performance of the IVS R1 and R4 sessions. Adv Space Res 73(1):317–336. https://doi.org/10.1016/j.asr.2023.07.020

Figure legends

Figure 1. Geographical distribution of AOV network stations. Potential future stations expected to participate in the network are shown in names with parenthesis.

Figure 2. Observing history of the 21 AOV stations. Each line shows the AOV sessions in chronological order, while each row represents the network station, red circles indicating that the station participated in the session. Key events during the period: TSUKUB32 was demolished at the end of 2016 (Ishimoto et al. 2017); HOBART12 replaced the receiver from S/X to VGOS in mid 2017 (McCallum et al. 2020); KASHIM11 and KASHIM34 were demolished in 2020 (Sekido and Kawai 2021a,b); USUDA64 and UCHINOUR joined the AOV in 2024 and 2025, respectively.

Figure 3. dUT1 formal uncertainties for AOV, R1, R4, AUSTRAL, EUROPE, and OHIGGINS sessions observed in the period after March 2015, when the first AOV session was conducted. Median values of dUT1 uncertainties in the same period are presented with lines for each type of session.

Figure 4. Same as Figure 3, but for X-pole.

Figure 5. Same as Figure 3, but for Y-pole.

Figure 6. Time series of station coordinates in the X, Y, and Z directions for the ISHIOKA, YARRA12M, and URUMQI stations. Station coordinates obtained from AOV sessions are marked with red circles. The vertical axes represent relative positions with those of the AOV001 session taken as zero.

Figure 7. Median values of uncertainties in the X, Y, and Z positions obtained from AOV sessions (red) and other sessions (gray) for stations which have results of more than one AOV session in this analysis.

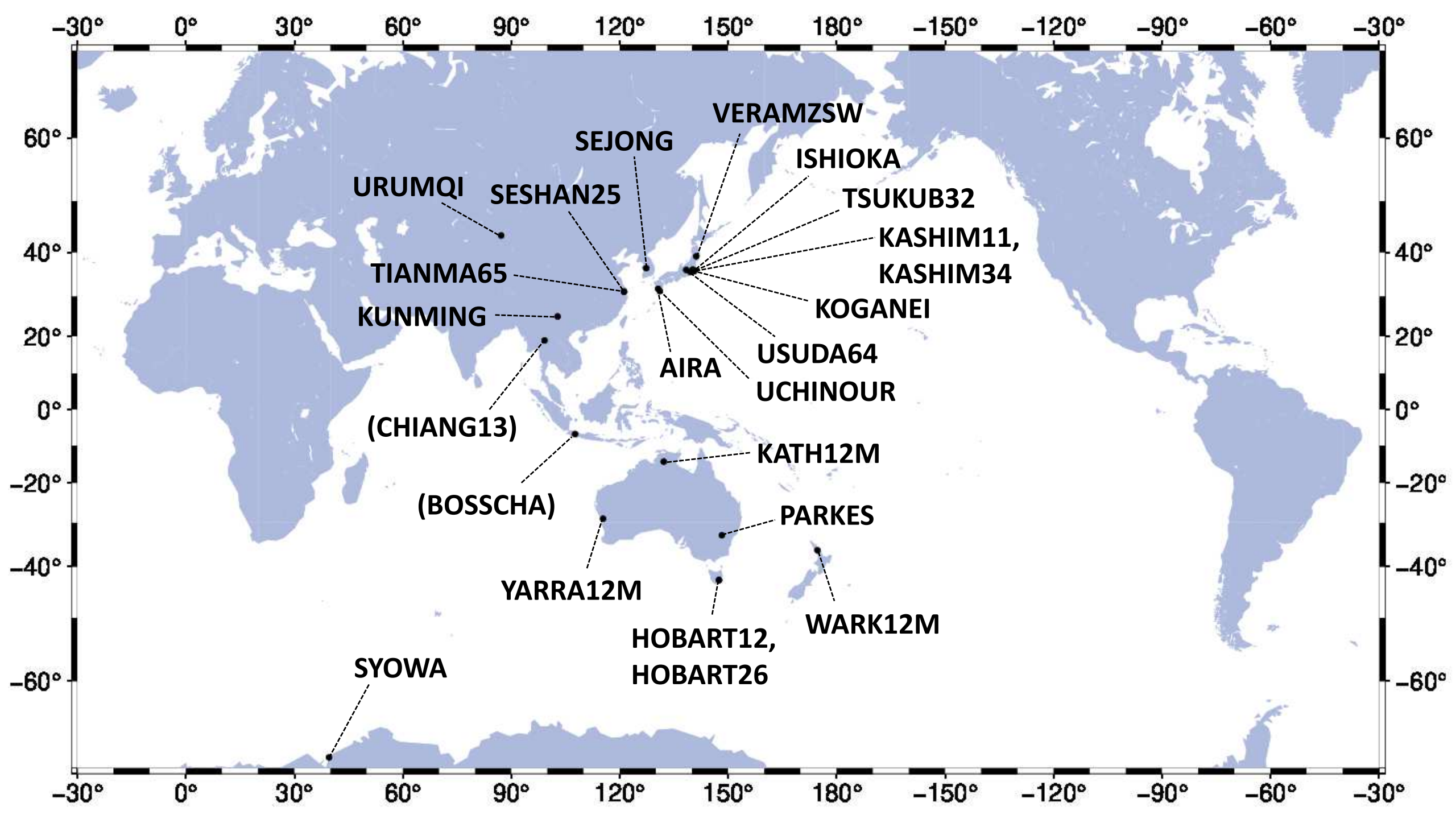
Figure 8. Baseline lengths repeatabilities (wrms) from the analysed sessions. We

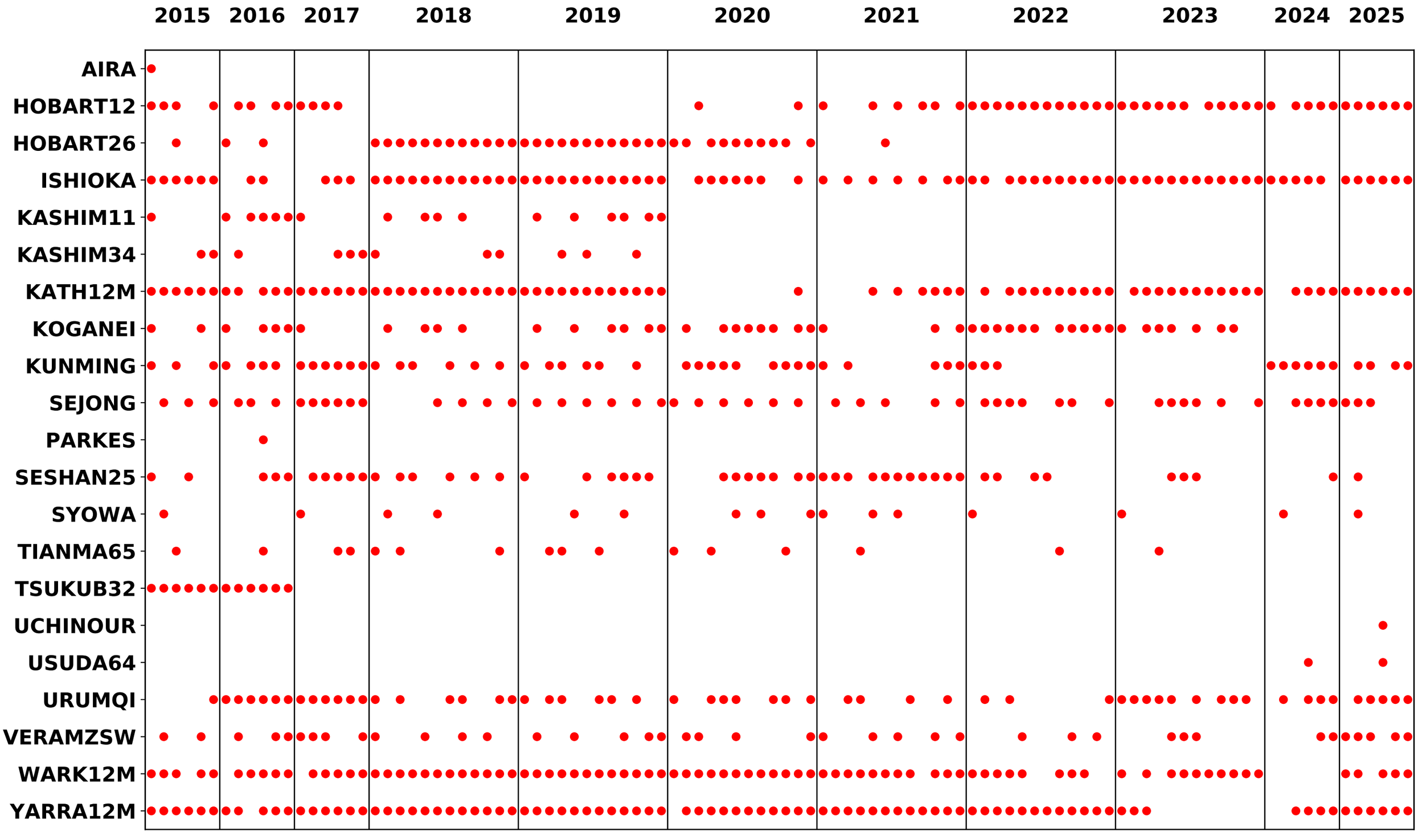
774 compare results from all alanysed IVS sessions (black crosses), only AOV sessions (red
775 circles) and R1 sessions (gray circles). The baseline SEJONG–SYOWA has a wrms of
776 189 mm in all IVS sessions and is displayed with a black star at the edge of the figure
777 at 60 mm wrms. The black bars show the differences between results (wrms) for the
778 AOV sessions compared to the whole dataset of all analysed sessions. Hereby, negative
779 values mean that the repeatability is lower (i.e. more precise) for AOV sessions. The red
780 and dashed black lines show linear fits to the AOV sessions and all IVS sessions,
781 respectively, excluding outliers with WRMS values larger than 50 mm.

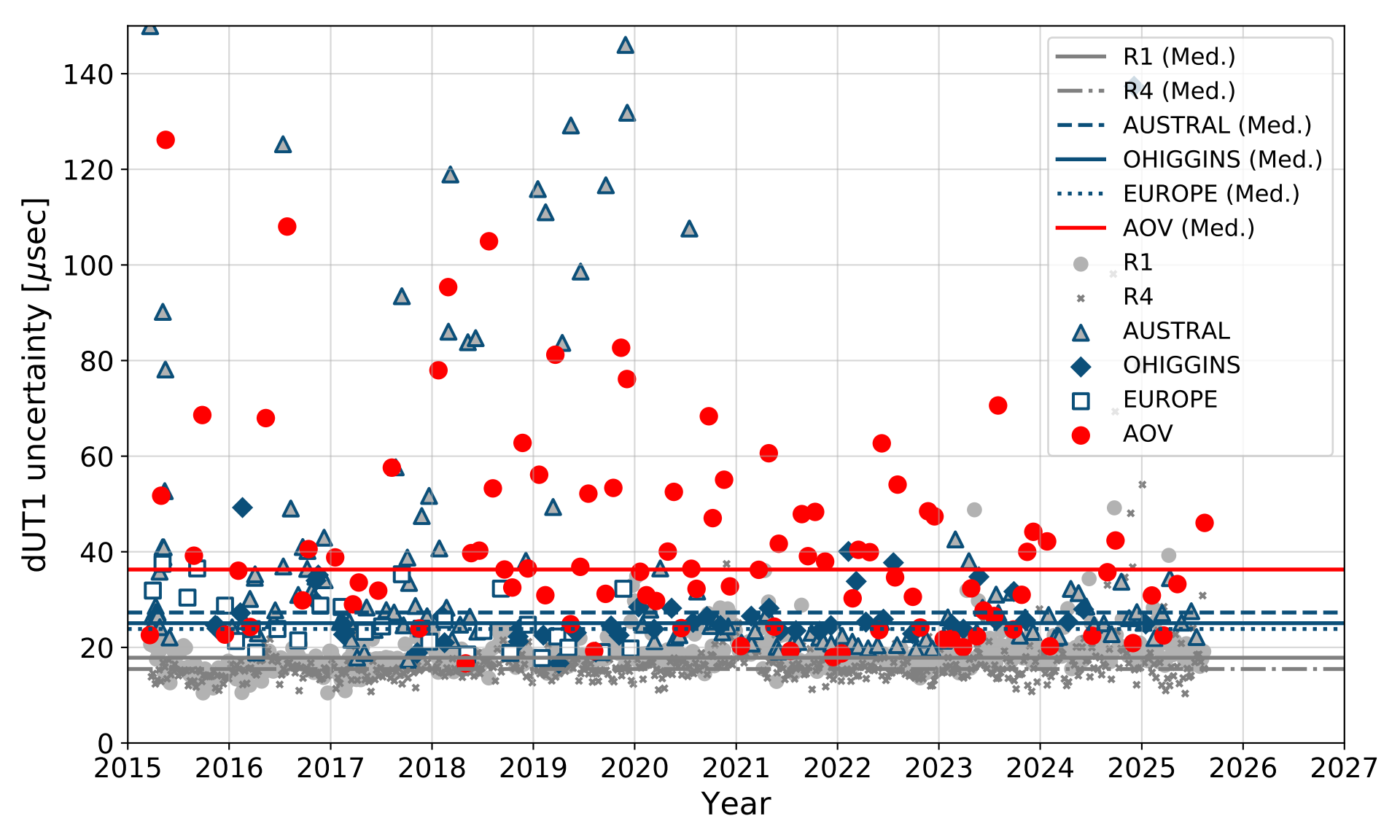
782 **Figure 9.** Simulated repeatability for X-pole, Y-pole and dUT1 values in AOV098 and
783 AOV100. EOP repeatabilities calculated with the current AOV network are shown in
784 gray bars, and those with expanded network including CHIANG13, BOSSCHA and
785 both of the stations are shown in blue bars.

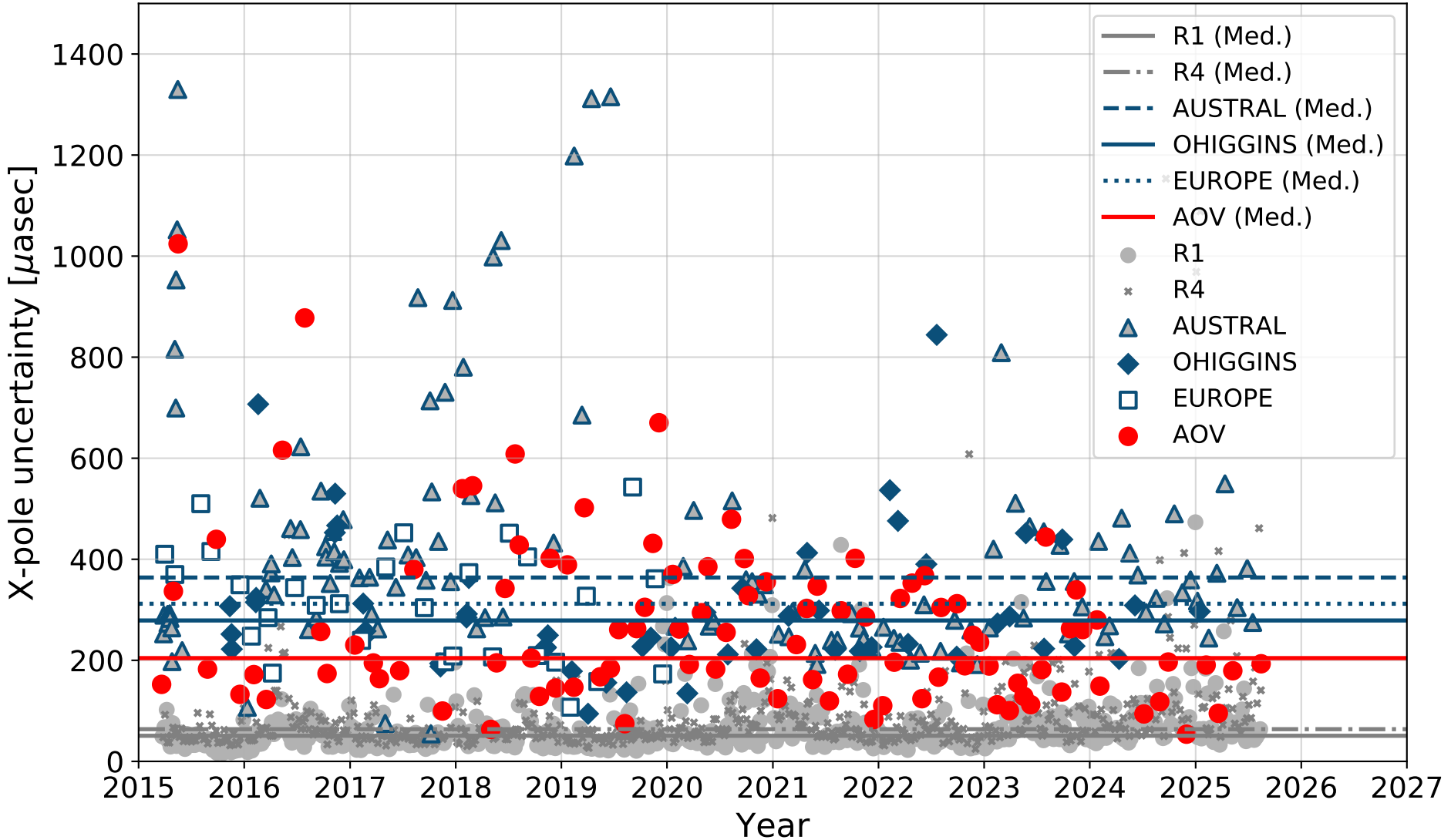
786 **Figure 10.** Simulated repeatability for X-pole, Y-pole, dUT1 and station positions for
787 ISHIOKA, HOBART12, KATH12M and YARRA12M in AOV098, AOV100 (S/X)
788 and VAO999 (VGOS).

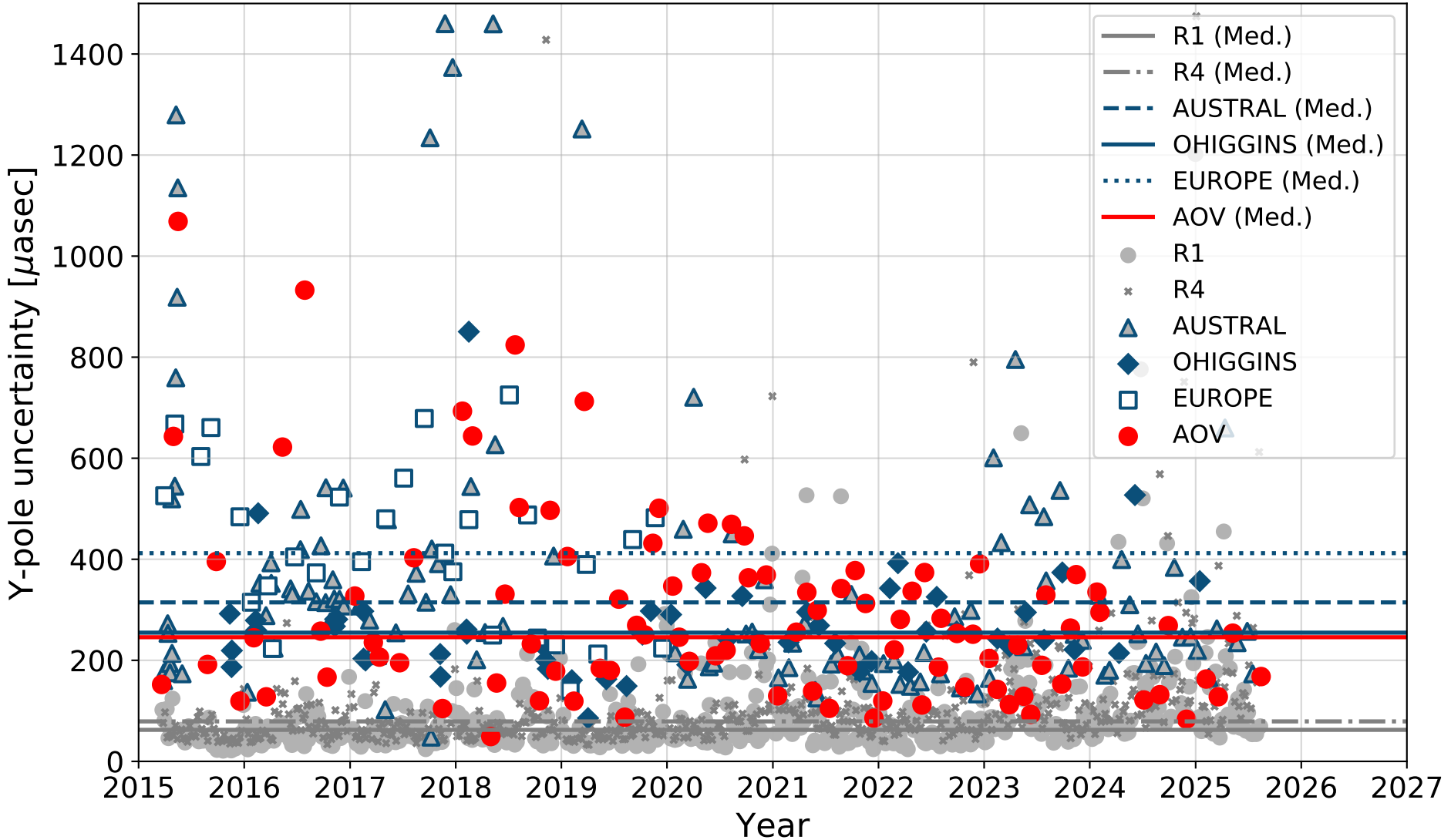
789


VERAMZSW
SEJONG
ISHIOKA
URUMQI
SESHAN25
TSUKUB32
KASHIM11,
KASHIM34
TIANMA65
KOGANEI
KUNMING
USUDA64
AIRA
UCHINOUR
(CHIANG13)
KATH12M
(BOSSCHA)
PARKES
YARRA12M
WARK12M
HOBART12,
HOBART26
SYOWA
−30°
0°
30°
60°
90°
120°
150°
180°
−150°
−120°
−90°
−60°
60°
40°
20°
0°
−20°
−40°
−60°


2015
2016
2017
2018
2019
2020
2021
2022
2023
2024
2025
AIRA
HOBART12
HOBART26
ISHIOKA
KASHIM11
KASHIM34
KATH12M
KOGANEI
KUNMING
SEJONG
PARKES
SESHAN25
SYOWA
TIANMA65
TSUKUB32
UCHINOUR
USUDA64
URUMQI
VERAMZSW
WARK12M
YARRA12M


R1 (Med.)
R4 (Med.)
AUSTRAL (Med.)
OHIGGINS (Med.)
EUROPE (Med.)
AOV (Med.)
R1
R4
AUSTRAL
OHIGGINS
EUROPE
AOV
dUT1 uncertainty [μsec]
Year
0
20
40
60
80
100
120
140
2015
2016
2017
2018
2019
2020
2021
2022
2023
2024
2025
2026
2027


R1 (Med.)
R4 (Med.)
AUSTRAL (Med.)
OHIGGINS (Med.)
EUROPE (Med.)
AOV (Med.)
R1
R4
AUSTRAL
OHIGGINS
EUROPE
AOV
X-pole uncertainty [μasec]
Year
0
200
400
600
800
1000
1200
1400
2015
2016
2017
2018
2019
2020
2021
2022
2023
2024
2025
2026
2027


R1 (Med.)
R4 (Med.)
AUSTRAL (Med.)
OHIGGINS (Med.)
EUROPE (Med.)
AOV (Med.)
R1
R4
AUSTRAL
OHIGGINS
EUROPE
AOV
Y-pole uncertainty [μasec]
Year
0
200
400
600
800
1000
1200
1400
2015
2016
2017
2018
2019
2020
2021
2022
2023
2024
2025
2026
2027

ISHIOKA

YARRA12M

URUMQI

X [mm]

Y [mm]

Z [mm]

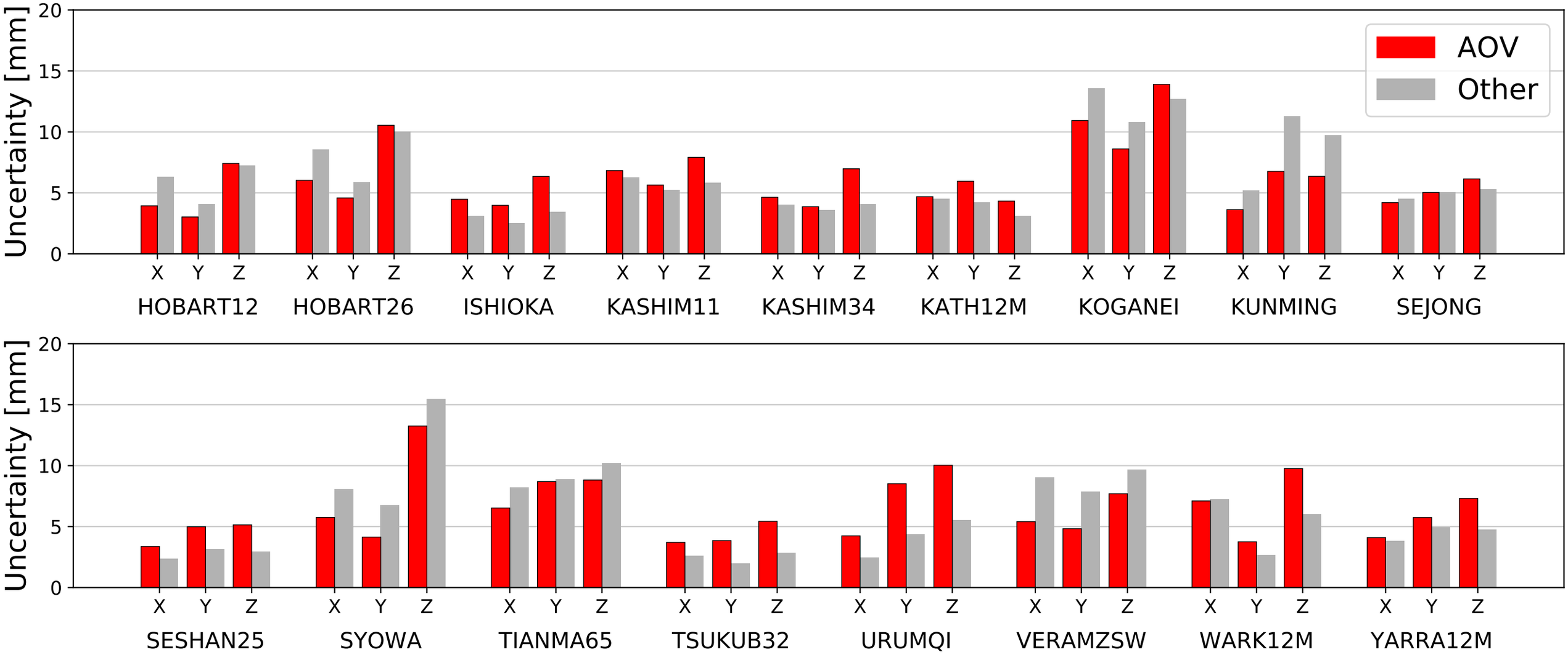
Other

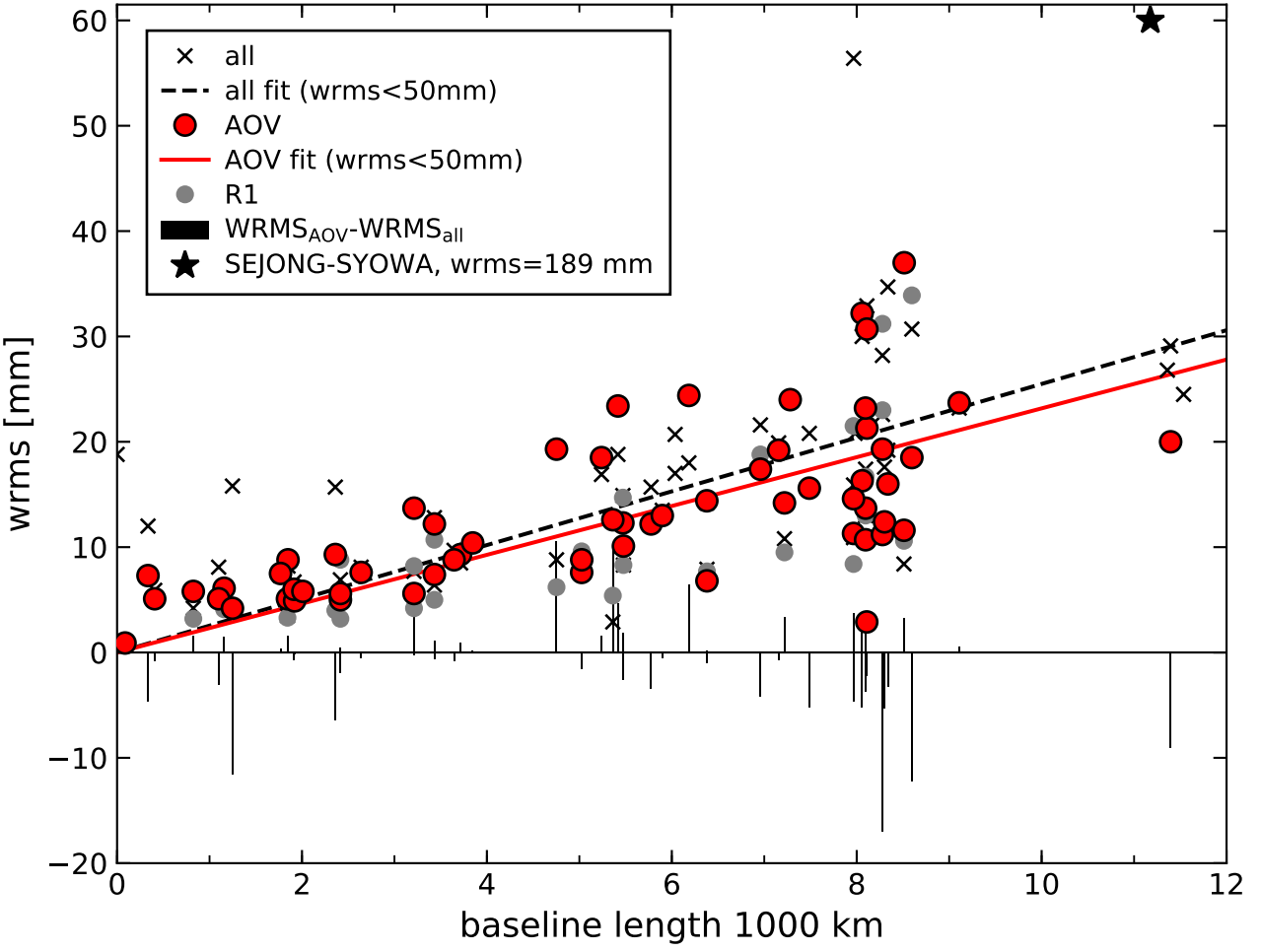
AOV

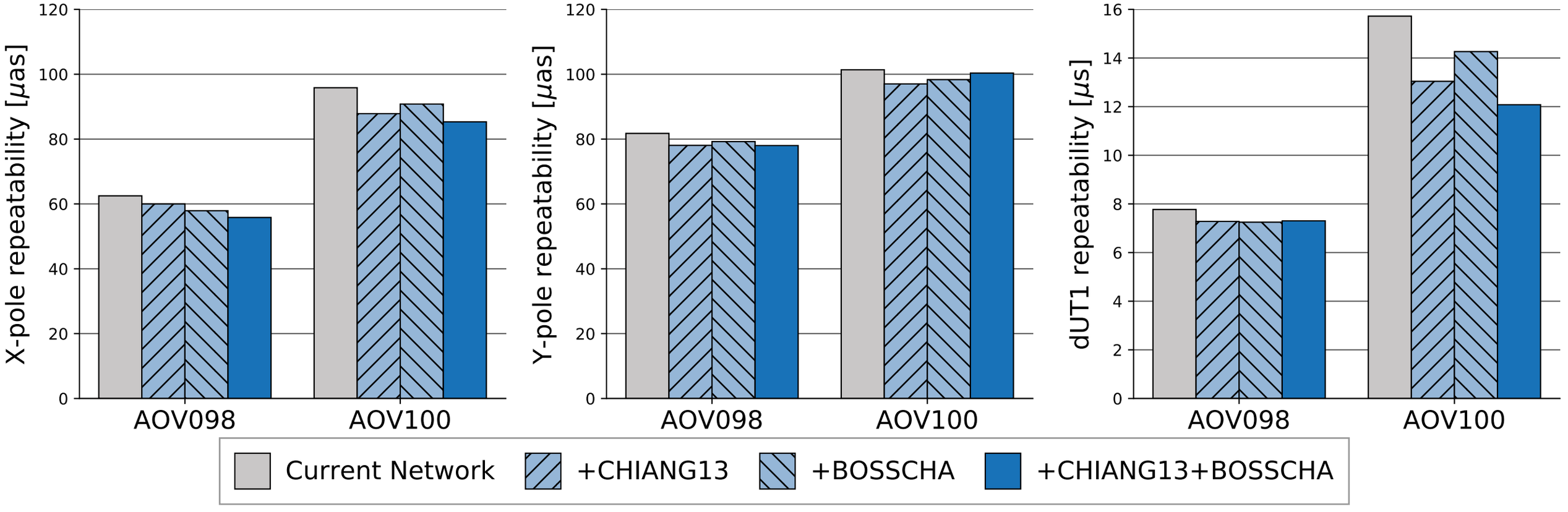
Year

Year

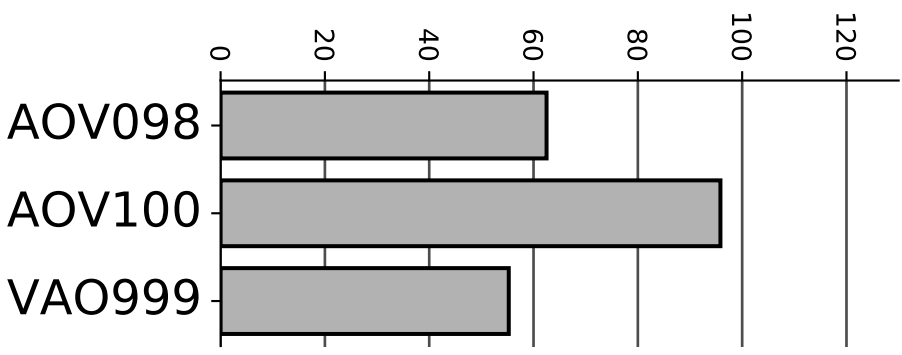
Year


Uncertainty [mm]
20
15
10
5
0
AOV
Other
X Y Z
HOBART12
HOBART26
ISHIOKA
KASHIM11
KASHIM34
KATH12M
KOGANEI
KUNMING
SEJONG
SESHAN25
SYOWA
TIANMA65
TSUKUB32
URUMQI
VERAMZSW
WARK12M
YARRA12M

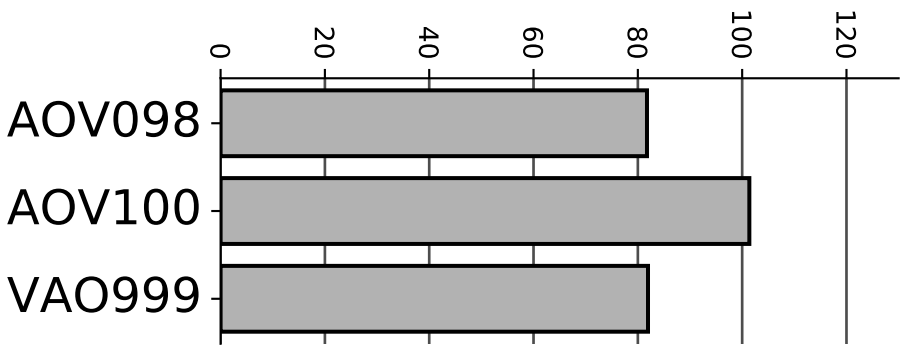

all
all fit (wrms<50mm)
AOV
AOV fit (wrms<50mm)
R1
WRMS$_{AOV}$-WRMS$_{all}$
SEJONG-SYOWA, wrms=189 mm
wrms [mm]
baseline length 1000 km
60
50
40
30
20
10
0
−10
−20
0
2
4
6
8
10
12


X-pole repeatability [μas]
120
100
80
60
40
20
0
AOV098
AOV100
Y-pole repeatability [μas]
120
100
80
60
40
20
0
AOV098
AOV100
dUT1 repeatability [μs]
16
14
12
10
8
6
4
2
0
AOV098
AOV100
Current Network
+CHIANG13
+BOSSCHA
+CHIANG13+BOSSCHA

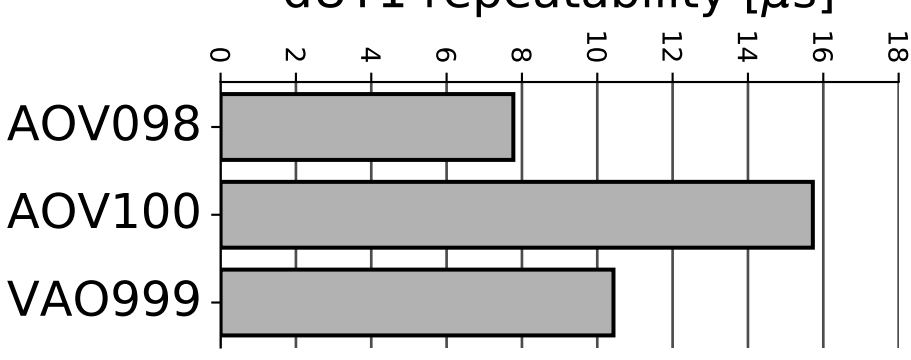
X-pole repeatability [μas]



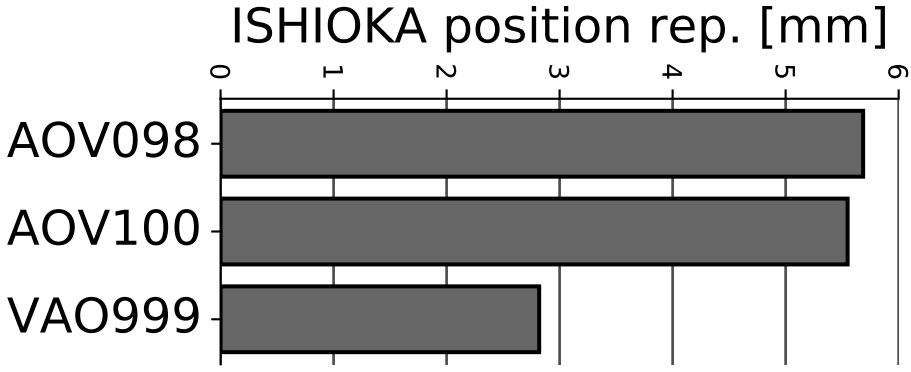
Y-pole repeatability [μas]



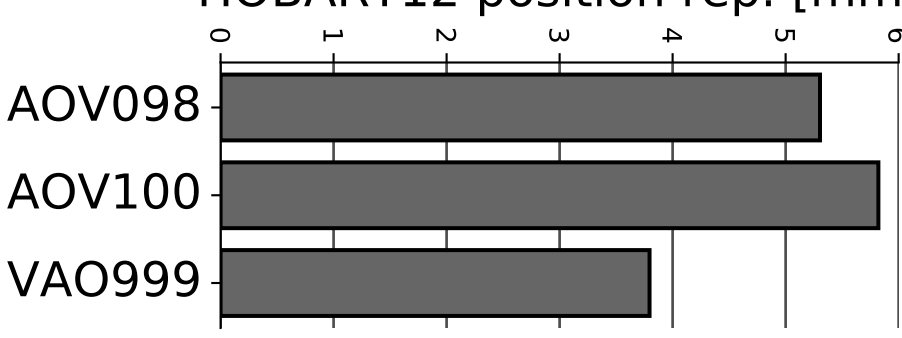
dUT1 repeatability [μs]



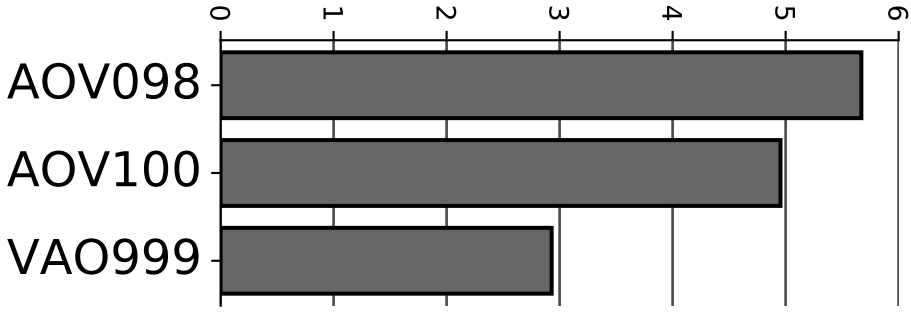
ISHIOKA position rep. [mm]



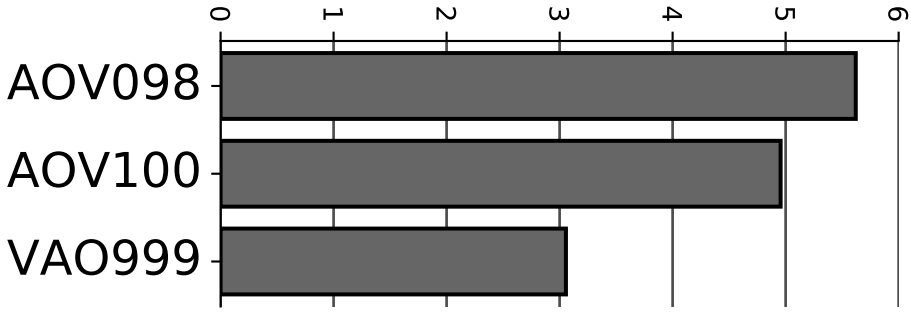
HOBART12 position rep. [mm]



KATH12M position rep. [mm]



YARRA12M position rep. [mm]



Supplementary Files

This is a list of supplementary files associated with this preprint. Click to download.

- graphicalabstract.png